Journal of Pharmaceutical and Biomedical Analysis 50 (2009) 570–575

Contents lists available at ScienceDirect

Journal of Pharmaceutical and Biomedical Analysis

journal homepage: www.elsevier.com/locate/jpba

Human serum albumin interaction with oxaliplatin studied by capillary isoelectric focusing with the whole column imaging detection and spectroscopic method

Tibebe Lemma, Janusz Pawliszyn*

Department of Chemistry, University of Waterloo, Waterloo, Ontario N2L 3G1, Canada

ARTICLE INFO

Article history:
Received 7 July 2008
Received in revised form 18 October 2008
Accepted 20 October 2008
Available online 5 November 2008

Keywords:
Capillary isoelectric focusing
Human serum albumin
Platinum anticancer drugs
Whole column imaging detection
Fluorescence
UV–vis absorbance

ABSTRACT

Capillary isoelectric focusing (CIEF) with whole column imaging detection (WCID) was used to investigate drug-protein interactions. This study was designed to examine the interaction between the platinum-based anticancer drug, oxaliplatin, with human serum albumin (HSA) in aqueous solution at physiological pH with drug concentrations of 10 to 100 μM and a constant concentration of HSA (5.0×10^{-5} M). The reaction mixtures were incubated for 0, 0.5, 1, 12, 24, 48 and 72 h at 37 °C in a water bath. The CIEF results indicate that with increasing the drug concentration, the complex formation of protein adducts increased compared to low-drug concentrations and major structural changes were observed as the incubation time progressed. The altered CIEF profile demonstrated the possible conformation change due to the binding of the drug. Results also showed a significant protein's p*I* shift for higher HSA–oxaliplatin incubation ratios. Furthermore, spectroscopic evidence shows that oxaliplatin caused the fluorescence quenching of HSA by formation of HSA–oxaliplatin complex. Using the Stern–Volmer equation, the quenching constants were calculated in the linear range. The quenching rate constants K_q at three different temperatures indicating the presence of static quenching mechanism in the interactions of oxaliplatin with HSA. This paper describes the validity of the CIEF-WCID technique for the study of protein–drug interactions and provides useful information and insight into the interaction of anticancer drugs with HSA.

© 2008 Elsevier B.V. All rights reserved.

1. Introduction

Capillary isoelectric focusing (CIEF) provides high-resolution separation of amphoteric biomolecular species based on differences of their isoelectric point in a pH gradient formed by carrier ampholytes when an electric potential is applied [1]. This high-throughput technique offers greater resolving power and has become a standard method for analysis of protein and protein–ligand interaction. The utilization of the whole column detection approach with UV whole column imaging detection (WCID) gives this separation technique a unique advantage over the conventional single point detection [1–4]. For example, in single point detection, several problems are encountered during the sample mobilization process, including protein precipitation, long analysis time and distortion of pH gradient. In contrast, CIEF-WCID successfully eliminates the mobilization process by using the WCID technique.

Thanks to the advantage of on-column detection and the capability of attaining real-time monitoring of the changes in peak area, CIEF-WCID is suitable for protein–protein and protein–drug interactions. Recently, CIEF-WCID has been successfully applied in our group to investigate protein–DNA [5], protein–amino acid [6] and protein–lipid [3,7–9] interactions. Furthermore, we demonstrated the use of this technique to determine the molecular weight of unknown proteins [10]. CIEF-WCID is expected to make a unique contribution in proteomic research because of its ability to resolve wide ranges of proteins and protein complexes that have small differences in p*I* in real-time. This technique is very important when one studies protein–ligand interactions such as protein–protein, protein–DNA and protein–drug.

The development of efficient and sensitive analytical methods for the separation, identification and quantification of drug–protein adducts is paramount for understanding the drug activity and toxicity. The objective of the present study is to develop a CIEF-WCID to investigate the interactions of platinum-containing anticancer drugs, namely oxaliplatin, with a model blood protein, human serum albumin (HSA). The structural changes of HSA are investigated by monitoring the p*I* during the incubation of oxaliplatin with HSA. CIEF is the highest efficiency, single-dimensional separation

* Corresponding author. Tel.: +1 519 888 4567; fax: +1 519 746 0435.
E-mail address: janusz@uwaterloo.ca (J. Pawliszyn).

0731-7085/$ – see front matter © 2008 Elsevier B.V. All rights reserved.
doi:10.1016/j.jpba.2008.10.028

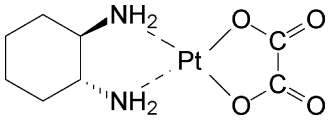

Fig. 1. Structure of oxaliplatin.

method available for the investigation of the interaction between proteins and ligands. This technique offers a number of advantages, including speed, high-separation efficiency, short analysis time and reduced sample consumption. Although the CIEF technique shows a number of advantages, quantitative information was chiefly provided by other techniques. In the present work, we demonstrated the development of CIEF-WCID technique association using fluorescence spectroscopy to investigate the interaction between HSA with oxaliplatin.

To our knowledge, the investigation of oxaliplatin interaction with HSA by CIEF with WCID is the first report of this type of analysis.

Platinum-based drugs are among the most active anticancer agents and have been widely used in the treatment of a variety of human tumors. Over the last 30 years, a large number of platinum analogues have been synthesized to enlarge the spectrum of activity, overcome cellular resistance and/or reduce the toxicity of both first (i.e. cisplatin) and second generation (i.e. carboplatin) platinum drugs [11]. Of these platinum-based compounds, oxaliplatin (Fig. 1), a novel compound containing a *trans*-1-(*R*, *R*)-1,2-diaminocyclohexane (DACH) carrier ligand, has recently been approved for the treatment of metastatic colorectal carcinoma in conjunction with fluoropyrimidines [12]. Oxaliplatin has shown *in vitro* and *in vivo* efficacy against many tumor cell lines and tumours, including those that are resistant to cisplatin and carboplatin [11,13–15]. In addition to its positive effects oxaliplatin also shows several toxic effects. The main cumulative dose-limiting toxicity of oxaliplatin is progressive peripheral sensory neuropathy [16,17]. It is also associated with an acute mild neuropathy, which reverses in several hours or days [16,17]. Oxaliplatin can also produce diarrhea, vomiting and haematological suppression [17–19]. However, the mechanisms of action and toxicity are not clear.

Platinum-containing anticancer drugs are believed to induce apoptosis in cancer cells by covalently binding to DNA [20–22], however, they also react with a number of proteins and peptides, such as glutathione, which may also play a role in detoxification of oxaliplatin [23]. In addition, after these drugs are introduced intravenously, 65–98% of the drugs are bound to blood plasma proteins [24–26], and 40% of the blood platinum is found in erythrocytes [26,27]. While it is widely accepted that platinum–DNA adducts are responsible for the drug's cytotoxicity, the role of platinum–protein adducts in the mechanism of action and toxicity of the drug remains unclear. Platinum–protein adducts are suggested to be the cause of the drug's side effects; however, there are also claims that they are important to the drug's activity [28]. Therefore, information on how anticancer drugs interact with proteins is important for the understanding of the mechanisms of action and toxicity of a drug and the optimization of cancer treatments.

HSA is an abundant protein that binds a variety of ligands with a typical concentration of 35–45 g l^{-1}. HSA interferes with certain antitumour drugs, changing their biological activity and affecting clinical activity [29]. In plasma, this protein is responsible for distributing and metabolizing many endogenous and exogenous ligands such as fatty acids, bilirubin, colic acid, metal ions, steroid hormones and pharmaceuticals, including metallodrugs [20,24,29,30–38]. HSA contains 585 amino acids and has a molecular weight of 66,500 Da. The crystal structure shows ligand binding sites located in the hydrophobic binding pockets in subdomains IIA and IIIA, each of which contains two subdomains (IA, IB, etc.) and is stabilized by 17 disulfide bridges and 1 free thiol at Cys-34 [39]. HSA contains a single tryptophan (Trp) residue in position 214 in subdomain IIA. At physiological pH (7.4), HSA presents two structural isomers: N and B. Ligand binding one of the domains (II or III) induces conformational changes on the other domain since both domains share a common interface. At pH 7.4, HSA tends to interact with positively charged species due to its negatively overall charge [40]. The molecular interaction between HSA with platinum-based anticancer agents have been extensively studied by variety of techniques [29–32,34,36,41,42].

In recent work, we investigated the effect of cisplatin and oxaliplatin on human hemoglobin [40] and described the adducts formation between the two analytes.

2. Experimental

2.1. Chemicals

Oxaliplatin (99.9%), carrier ampholytes (Pharmalytes 3.0-10.0) and HSA were purchased from Sigma (St. Louis, MO, USA). Polyvinylpyrrolidone (pvp) was purchased from Aldrich (Milwaukee, WI, USA). Water was purified with a NANOpure water system (Barnstead/Thermolyne, Dubuque, IA, USA) and had a minimum resistivity of 18.0 MΩ cm. All of the chemicals employed in this study were of analytical reagent and used without further purification.

2.2. Solutions and sample preparation

Stock solutions of oxaliplatin (*trans*-1-(*R*, *R*)-1,2-diaminocyclohexane (DACH) oxalatoplatinum) were prepared to a concentration of 5 mM. The HSA stock solution was prepared to a concentration of 25 μM. The stock solutions were freshly prepared everyday. All reaction mixtures were prepared in duplicate.

2.2.1. Incubation of HSA with oxaliplatin

Samples containing a physiological concentration of HSA (5.0×10^{-5} M), tryptophan (5.0×10^{-5} M) and different concentrations of oxaliplatin (0–100 μM) were incubated at 37 °C in a phosphate buffer solution (0.1 M pH 7.4) containing 10 M NaCl for a maximum of 3 days. The pH values of all of the reaction mixtures were maintained at 7.4 to mimic physiological conditions. The molar ratios of the incubated protein:drug solutions were 1:1, 1:10, 1:50 and 1:100, respectively. Aliquots were taken for analysis after 0, 0.5, 1, 2, 6, 12, 24, 48 and 72 h.

2.3. CIEF system

The CIEF experiments were pursued with a commercial iCE_{280} instrument (Convergent Bioscience, Mississauga, Ont., Canada). The system was equipped with a charge couple device (CCD) camera for image collection. Separations were performed on commercial cartridges with silica capillary tubes (Convergent Bioscience), with an effective length of 5 cm, 100 μm ID and 200 μm OD. The capillary wall was coated with fluorocarbon (Restek, Bellefonte, PA, USA) to suppress the electroosmotic flow (EOF). Focusing was carried out for 2 min at 500 V and the system was set at 3000 V for the remainder of the analysis. The catholyte and anolyte contained 1% pvp with 100 mM NaOH and 100 mM of H_3PO_4, respectively. The sample, which was mixed with 0.5% pvp and 2% ampholyte (pH 3–10), was manually injected with a needle. To avoid the inconsistent coating efficiency, all capillaries were dynamically coated with additives for 30 min prior to the experiment. During the focusing

process, the current was decreased from 10.8 to 4.7 μA, prior to completion.

2.4. Fluorescence quenching measurement

The fluorescence emission spectra of HSA in the presence of oxaliplatin were recorded on a PTI QuantaMaster Instrument equipped with a xenon lamp source and 1.0 cm quartz cell with a thermostat bath. Fluorescence quenching spectra were collected by recording the fluorescence emission wavelength from 300 to 500 nm at an excitation wavelength of 390 nm, and with the slit width 5.0 nm. Freshly prepared HSA and oxaliplatin solutions were mixed in 1:*n* ratios as previously described.

3. Results and discussion

3.1. CIEF investigation of oxaliplatin–HSA interaction

We have developed a CIEF technique to investigate the adduct formation between HSA and oxaliplatin in aqueous media, mimicking physiological conditions. The standard CIEF profile of HSA showed one peak (Fig. 2). The focusing time took 8 min. Within the 8 min focusing time, no peak distortion or intensity changes were observed. However, the peak area gradually started changing with a minor increase of the incubation ratio, and with higher oxaliplatin concentrations, the peaks altered drastically and diminished, which indicates the adduct formation between the two analytes. Figs. 2 and 3 show typical CIEF separation profiles for HSA (control) and HSA–oxaliplatin adducts in buffer solution. This result is in excellent agreement with previous hemoglobin-oxaliplatin studies, which demonstrated that oxaliplatin induces structural alterations when incubated with proteins.

Fig. 2 illustrates drug-free HSA (control) separated by CIEF containing two p*I* markers (4.65 and 7.05). It should be mentioned that the two p*I* markers were used to observe possible p*I* shifts during the incubation progress. In the absence of the drug, the electropherogram of HSA contains only one distinct peak, which is characteristic of this protein. The p*I* value of the HSA is approximately 5.7. However, a minor fluctuation can be observed due to an inconsistency in the manufacturing of the separation cartridges and focusing time. As shown in Fig. 3(a), no significant change was observed for the first 6 h of the incubation period. However, as the incubation time progressed from 6 to 12 h, the peak intensity started to decrease accompanying on increase in peak width of the profile. A small p*I* shift is also observed in going from a 12 to 72 h incubation time; this is most likely due to the early stage of adduct formation between the two analytes, accompanying the alteration of HSA surface properties.

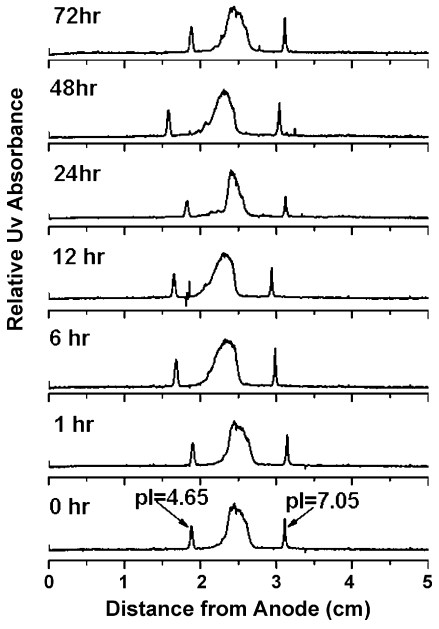

Fig. 2. The CIEF analysis of HSA (10 μM) incubated for 72 h at 310 K. For the CIEF analysis, a sample solution (400 μl) containing 2% pharmalytes (pH 3.0–10.0), p*I* markers (p*I* 6.14 and 8.40) and 0.5% PVP was injected into the capillary by pressure using a syringe. The catholyte and anolyte were 100 mM NaOH and H_3PO_4 consecutively. The focusing voltage was set at 500 V for 2 min and 3000 V for the remainder of the focusing period. The observed p*I* variations may arise from small changes of the capillary inner wall properties during successive runs.

The CIEF profile for the reaction mixtures that contain HSA–oxaliplatin (1:1, 1:10, 1:50 and 1:100 molar ratios) is shown in Fig. 3(a)–(d). From Fig. 3(a), it is seen that as the incubation ratio reached 12 h, the area of the CIEF profile of HSA increased, which indicates the stage at which the adducts start forming between the two analytes. However, the profile indicates no p*I* shift or structural change within the 72 h incubation time. This indicates that the structural change was less evident at low-drug concentration. From Fig. 3(a), we also observed that the CIEF profiles are identical to that obtained in Fig. 2.

Fig. 3(b)–(d) shows the CIEF profile of HSA–oxaliplatin adducts in 1:10, 1:50 and 1:100 molar ratios, incubated at 37 °C under the same CIEF conditions. The spectral profile of Fig. 3(b) (1:10 molar ratio) shows the protein was markedly affected by the complexation with oxaliplatin. For short incubation times (0–6 h), in contrast to Figs. 2 and 3(a), a minor p*I* shift was observed after 1 h of incubation. Also shown in Fig. 3(b) is the increase of spectral width. When the incubation time progressed from 1 to 72 h, the relative intensity of the peaks was decreasing as a function of incubation time. Although the p*I* shift was not significantly changed between the time frame of 12–72 h, the drug induced structural alteration of the protein structure. This demonstrates the stage at which the adducts are formed between the two analytes. The decreasing intensity and increasing area of the CIEF profiles further demonstrate the effect of the drug on the protein structure.

The pattern of the electropherograms recorded for samples containing 1:50 and 1:100 molar ratio of HSA–oxaliplatin showed substantial differences from the other samples (1:1 and 1:10 molar ratio). As shown in Fig. 3(c) and (d), there is a concentration and time-dependent CIEF profile alteration and structural breaking down into fragments, or forming aggregates of the protein adducts. Although similar CIEF profiles were observed for the two incubation ratios, the degradation kinetics shows a minor difference between the two samples. In the case of Fig. 2(c) (1:50), the distortion of the protein adducts started after 6 h of incubation time, followed by peak shape changes. These are the expected results since the sample contains a smaller amount of oxaliplatin compared to that of the 1:100 ratio. It can also be seen that the CIEF profile exhibits p*I* shift, suggesting that adducts form between the two analytes. As time progressed, the adducts formed completely dissociated after 12 h of incubation time, which suggests that the drug-protein ratios are approaching saturation of the protein binding sites. Previously, we had shown that there is a biologically significant interaction between protein (Hb A) and oxaliplatin [40]. Similar behavior was observed when oxaliplatin incubated with Hb at the two ratios (1:50 and 1:100). However, for 1:100 molar ratio, the dissociation of the adducts starts after 6 h, which suggested that the kinetic transformation was faster compared with the lower molar ratio (1:50). These two samples show very different behavior under the same separation conditions. One of the significant differences between the two samples was the relatively broader peak shape for the 1:100 molar ratios. This broader peak starts appearing

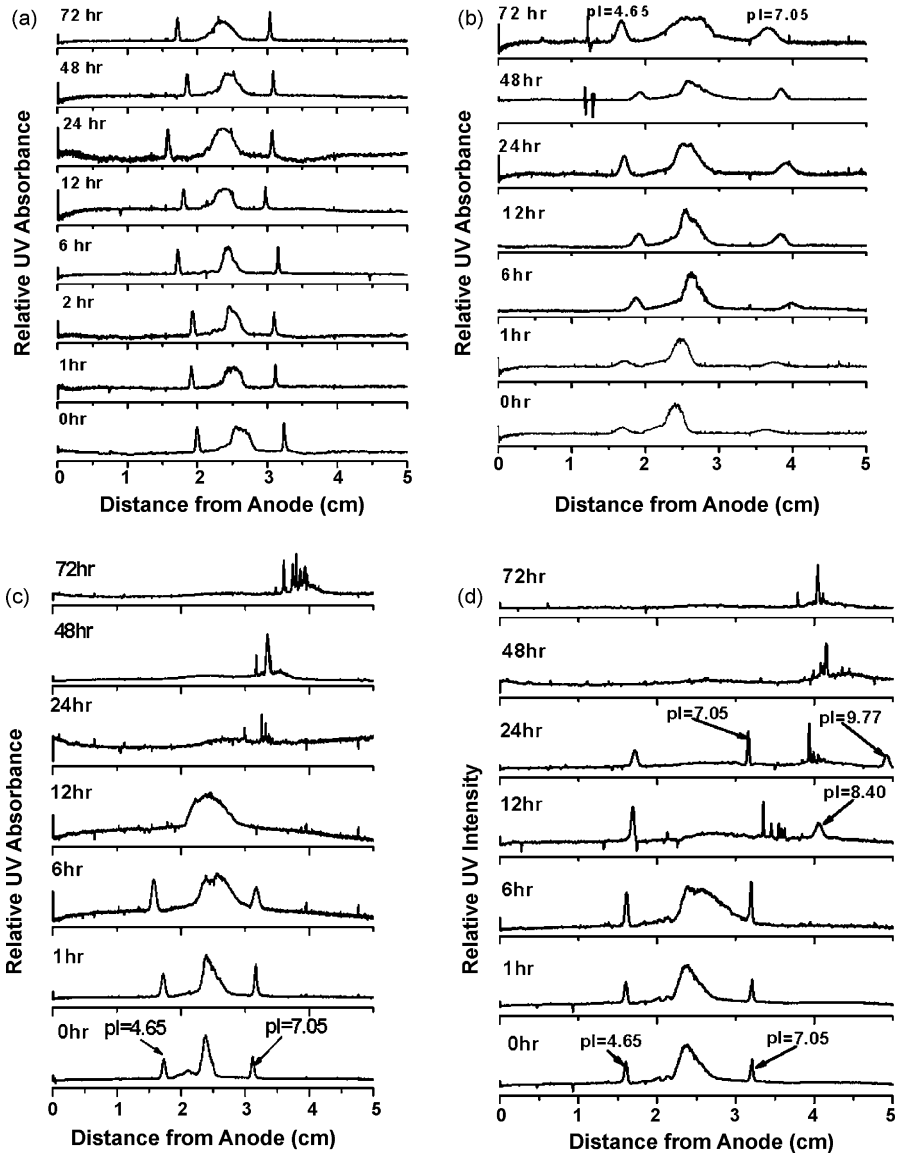

Fig. 3. Electropherograms representative of binding of HSA with oxaliplatin: (a) 1:1, (b) 1:10, (c) 1:50 and (d) 1:100 molar ratios. The drug-protein mixtures were incubated for 3 days at 310 K. Appropriate amounts of the incubated samples were removed and mixed with 0.5% PVP, 2% pharmalytes (pH 3.0–10.0) and p*I* markers (4.65, 7.05, 8.40 and 9.77) for each CIEF run. Catholyte and anolyte were 100 mM NaOH and H_3PO_4. On electropherogram (c) and (d), the p*I* markers were not mixed with the running sample due the formation of fragments after 24 and 48 h incubation time. For all solutions, the total concentration of HSA was constant: 5.0×10^{-5} M. The separation conditions are described in Fig. 1.

after approximately 1 h of incubation time. When the incubation time reached 12 h, the peak almost disappeared and the fragments of the adducts appeared. One possible explanation was that the formed adduct was breaking down or changing to other species as incubation time progressed. It has been shown in a number of previous studies that HSA contains platination sites such as Met, His, or S–S bonds [34]. Since the S–S bridge is responsible for the stabilization of HSA, a high concentration of oxaliplatin might cleave the S–S bridge. This may lead to the activation of the protein aggregate, which was observed in our experiments for the two higher incubation ratios (1:50 and 1:100).

3.2. Fluorescence quenching spectra and quenching mechanism

Fluorescence quenching can be described by the Stern–Volmer equation [43]:

$$\frac{F_0}{F} = 1 + K_q\tau_0[Q] = 1 + K_{SV}[Q] \quad (1)$$

where F_0 and F are the fluorescence intensities in the absence and presence of the quencher, K_q represents the quenching rate constant, K_{SV} the Stern–Volmer dynamic quenching constant, τ_0 (10^{-8} s) [44] the average lifetime of the biomolecule without quencher, and [*Q*] is the concentration of the quencher respectively. The K_{SV} and K_q values are calculated from the linear plot of F_0/F against the drug concentration, [*Q*]:

$$K_q = \frac{K_{SV}}{\tau_0} \quad (2)$$

There are two kinds of fluorescence quenching: dynamic and static. These two mechanisms can be distinguished from each other by their differing dependences on temperature and excited-state lifetime. The K_{sv} value decreases with an increase in temperature for static quenching, but there is a reverse effect on dynamic quenching. For higher temperatures, the diffusion constant increases, due to the dissociation of weakly bonded complexes. It is well known that the maximum scattering collision quenching constant

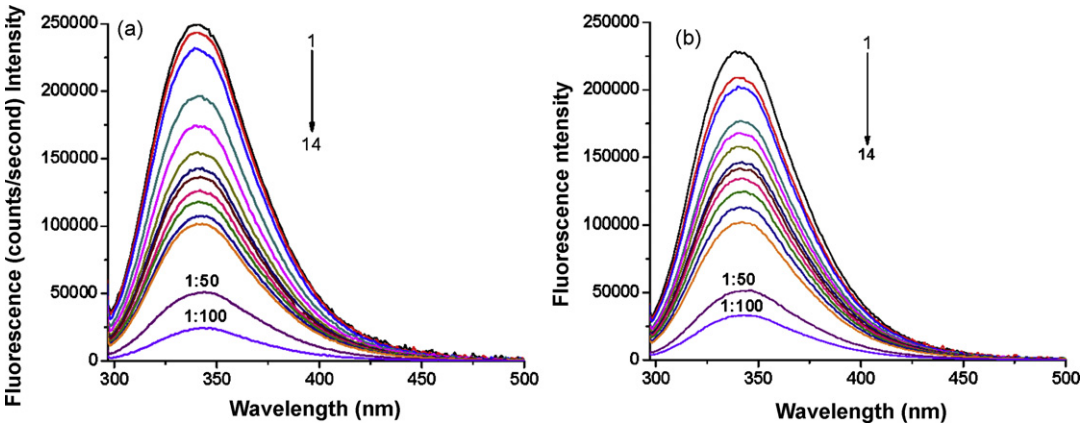

Fig. 4. Fluorescence spectra of HSA (5.0×10^{-5} M): different concentrations of oxaliplatin: curves (1)–(14), 0, 1.0, 2.0, 4.0, 6.0, 8.0, 10.0, 12.0, 14.0, 16.0, 18.0, 20.0, 50.0 and 100.0, respectively: (a) 298 K, (b) 310 K.

Table 1
Stern–Volmer dynamic quenching constants and quenching rate constant of HSA and oxaliplatin at different temperatures.

pH	T (K)	K_{SV} (l mol^{-1})	K_q (l mol^{-1} s^{-1})	R
7.40	298	1.480×10^3	1.480×10^{11}	0.997
7.40	310	1.120×10^3	1.120×10^{11}	0.993
7.40	320	1.089×10^3	1.089×10^{11}	0.996

of various quenchers with biological macromolecules is about 2.0×10^{10} l mol^{-1} s^{-1}. For HSA–oxaliplatin as shown in Table 1, the quenching constant is much higher than 2.0×10^{10} l mol^{-1} s^{-1}. The K_{sv} decrease with temperature increased. Therefore, it can be concluded that the quenching was not initiated by dynamic collision but probably initiated by static quenching resulting from complex formation between HSA–oxaliplatin.

Figs. 4–6 show the fluorescence emission spectra for HSA with various molar ratios of oxaliplatin at pH 7.4, excited at 290 nm and the Stern–Volmer plot, respectively. As the data shows, the fluorescence spectra of HSA progressively decreased with the increasing concentration of oxaliplatin. These observations can be rationalized in terms of interactions between oxaliplatin and HSA and formation of complexes between the two analytes.

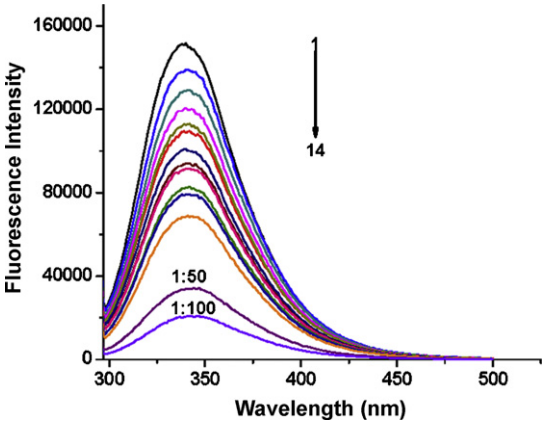

Fig. 5. Fluorescence spectra of HSA (5.0×10^{-5} M) in the present of different concentration of oxaliplatin at 320 K: curves (1)–(14), 0, 1.0, 2.0, 4.0, 6.0, 8.0, 10.0, 12.0, 14.0, 16.0, 18.0, 20.0, 50.0 and 100.

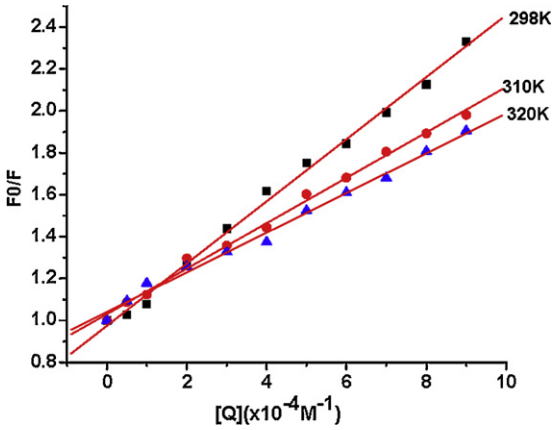

Fig. 6. Stern–Volmer plot for the binding of HSA–oxaliplatin at different temperatures (298, 310 and 320 K).

4. Conclusion

CIEF-WCID allows us to monitor the p*I* shift and structural alteration of the protein, when interacted with ligands such as the anticancer agents (oxaliplatin). Several conclusions can be drawn from the results presented here. First, the experimental results demonstrate the significant effects of oxaliplatin on the structural stability of HSA when incubated for a maximum 72 h at physiological pH. Second, on the basis of the data presented here, it may be hypothesized that oxaliplatin may have multiple binding sights on HSA, and, at higher molar ratios, oxaliplatin may cleave the S–S bond, which is responsible for the stability of the protein. Previous work suggested that cisplatin, the *another* platinum-based anticancer drug, interacts with multiple sights on HSA when incubated with the protein [42]. Furthermore, quenching of the intrinsic fluorescence of HSA reinforces the formation of the HSA–oxaliplatin complex.

Finally, CIEF-WCID can help to elucidate the anticancer mode of action regarding the affinity toward proteins. However, the technique can be considered as a complementary rather than a competitive technique, because the method exhibits specific ranges of applicability, advantages and disadvantages. For instance, with nano-ESI-MS/MS, the dissociation constant and binding sites may be determined, while with CIEF only adduct formations and p*I* shifts are observed.

Acknowledgments

The author would like to thank Dr. Michael Palmer for the use of his equipment.This work was supported by the Natural Sciences and Engineering Research Council of Canada (NSERC) and Convergent Bioscience Ltd.

References

[1] S. Hjerten, M.D. Zhu, J. Chromatogr. 346 (1985) 265–270.
[2] Z. Liu, J. Pawliszyn, Anal. Chem. 75 (2003) 4887–4894.
[3] T. Bo, J. Pawliszyn, Anal. Chim. Acta 559 (2006) 1–8.
[4] J. Reedijk, Chem. Commun. (1996) 801–806.
[5] Z. Liu, A.P. Drabovich, S.N. Krylov, J. Pawliszyn, Anal. Chem. 79 (2007) 1097–1100.
[6] T. Bo, J. Pawliszyn, J. Chromatogr. A 1105 (2006) 25–32.
[7] T. Bo, J. Pawliszyn, J. Sep. Sci. 29 (2006) 1018–1025.
[8] T. Bo, J. Pawliszyn, Anal. Biochem. 350 (2006) 91–98.
[9] T. Bo, J. Pawliszyn, Electrophoresis 27 (2006) 852–858.
[10] Z. Liu, T. Lemma, J. Pawliszyn, J. Proteom. Res. 5 (2006) 1246–1251.
[11] E. Cvitkovic, Semin. Oncol. 25 (1998) 1–3.
[12] M.A. Graham, G.F. Lockwood, D. Greenslade, S. Brienza, M. Bayssas, E. Gamelin, Clin. Cancer Res. 6 (2000) 1205–1218.
[13] E. Cvitkovic, Br. J. Cancer 77 (1998) 8–11.
[14] T.A. Dunn, H.J. Schmoll, V. Gruenwald, C. Bokemeyer, J. Casper, Invest. New Drugs 15 (1997) 109–114.
[15] P. Soulie, A. Bensmaine, C. Garrino, P. Chollet, E. Brain, M. Fereres, C. Jasmin, M. Musset, J.L. Misset, E. Cvitkovic, Eur. J. Cancer 33 (1997) 1400–1406.
[16] E. Gamelin, A. Le Bouil, M. Boisdron-Celle, A. Turcant, R. Delva, A. Cailleux, A. Krikorian, S. Brienza, E. Cvitkovic, J. Robert, F. Larra, P. Allain, Clin. Cancer Res. 3 (1997) 891–899.
[17] P.J. O'Dwyer, J.P. Stevenson, S.W. Johnson, Drugs 59 (2000) 19–27.
[18] C. Louvet, T. Andre, J.M. Tigaud, E. Gamelin, J.Y. Douillard, R. Brunet, E. Francois, J.H. Jacob, D. Levoir, A. Taamma, P. Rougier, E. Cvitkovic, A. de Gramont, J. Clin. Oncol. 20 (2002) 4543–4548.
[19] W. Kern, B. Beckert, N. Lang, J. Stemmler, M. Beykirch, J. Stein, E. Goecke, T. Waggershauser, J. Braess, A. Schalhorn, W. Hiddemann, Ann. Oncol. 12 (2001) 599–603.
[20] A. Eastman, Biochemistry 21 (1982) 6732–6736.
[21] E.R. Jamieson, S.J. Lippard, Chem. Rev. 99 (1999) 2467–2498.
[22] R.S. Go, A.A. Adjei, J. Clin. Oncol. 17 (1999) 409–422.
[23] A. Kung, D.B. Strickmann, M. Galanski, B.K. Keppler, J. Inorg. Biochem. 86 (2001) 691–698.
[24] J.J. Gullo, C.L. Litterst, P.J. Maguire, B.I. Sikic, D.F. Hoth, P.V. Woolley, Cancer Chemother. Pharmacol. 5 (1980) 21–26.
[25] M. Boisdron-Celle, A. Lebouil, P. Allain, E. Gamelin, Bull. Cancer 88 (Spec. No.) (2001) S14–S19.
[26] L. Pendyala, P.J. Creaven, Cancer Res. 53 (1993) 5970–5976.
[27] D.K. Rai, B. Landin, G. Alvelius, W.J. Griffiths, Anal. Chem. 74 (2002) 2097–2102.
[28] E. Espinosa, J. Feliu, P. Zamora, M. Gonzalez Baron, J.J. Sanchez, A. Ordonez, J. Espinosa, Lung Cancer 12 (1995) 67–76.
[29] I. Takahashi, T. Ohnuma, S. Kavy, S. Bhardwaj, J.F. Holland, Br. J. Cancer 41 (1980) 602–608.
[30] N. Ohta, D. Chen, S. Ito, T. Futo, T. Yotsuyanagi, K. Ikeda, Int. J. Pharmacol. 118 (1995) 85–93.
[31] A.I. Ivanov, J. Christodoulou, J.A. Parkinson, K.J. Barnham, A. Tucker, J. Woodrow, P.J. Sadler, J. Biol. Chem. 273 (1998) 14721–14730.
[32] J.F. Neault, H.A. Tajmir-Riahi, Biochim. Biophys. Acta 1384 (1998) 153–159.
[33] D. Gibson, C.E. Costello, Eur. J. Mass Spectrom. 5 (1999) 501–510.
[34] B.P. Esposito, R. Najjar, Coord. Chem. Rev. 232 (2002) 137–149.
[35] A.R. Timerbaev, S.S. Aleksenko, K. Polec-Pawlak, R. Ruzik, O. Semenova, C.G. Hartinger, S. Oszwaldowski, M. Galanski, M. Jarosz, B.K. Keppler, Electrophoresis 25 (2004) 1988–1995.
[36] A. Warnecke, I. Fichtner, D. Garmann, U. Jaehde, F. Kratz, Bioconjug. Chem. 15 (2004) 1349–1359.
[37] A.V. Rudnev, S.S. Aleksenko, O. Semenova, C.G. Hartinger, A.R. Timerbaev, B.K. Keppler, J. Sep. Sci. 28 (2005) 121–127.
[38] R. Timerbaev Andrei, G. Hartinger Christian, S. Aleksenko Svetlana, K. Keppler Bernhard, Chem. Rev. 106 (2006) 2224–2248.
[39] X.M. He, D.C. Carter, Nature 358 (1992) 209–215.
[40] T. Lemma, R. Mandal, X.-F. Li, J. Pawliszyn, J. Sep. Sci. 31 (2008).
[41] Y.-P. Tzeng, C.-W. Shen, T. Yu, J. Chromatogr. A 1193 (2008) 1–6.
[42] L. Trynda-Lemiesz, H. Kozlowski, B.K. Keppler, J. Inorg. Biochem. 77 (1999) 141–146.
[43] K. Ohyama, N. Kishikawa, H. Nakagawa, N. Kuroda, M. Nishikido, M. Teshima, H. To, T. Kitahara, H. Sasaki, J. Pharm. Biomed. Anal. 47 (2008) 201–206.
[44] J.R. Lakowicz, G. Weber, Biochemistry 12 (1973) 4161–4170.